Analyzing the brainstem circuits for respiratory chemosensitivity in freely moving mice

Amol Bhandare, Robert Huckstepp, Nicholas Dale.

School of Life Sciences, University of Warwick, Coventry, UK

Corresponding Author Email: n.e.dale@warwick.ac.uk

Abstract

The regulated excretion of CO_2 during breathing is a key life-preserving homeostatic mechanism. In the rostral medulla oblongata, neurons in two nuclei -the retrotrapezoid nucleus (RTN) and the rostral medullary raphe -have been proposed as central CO_2 chemosensors that mediate adaptive changes in breathing. Using synapsin promoter-driven expression of GCaMP6 and head-mounted mini-microscopes, we imaged the Ca^{2+} activity of RTN and raphe neurons in awake adult mice during inspiration of elevated CO_2. 40% of raphe neurons were activated by 3% and 6% inspired CO_2. By contrast, only 5% of RTN neurons were activated by CO_2. 4% of RTN neurons were inhibited by elevated CO_2, and 4% of RTN neurons were coactive with exploratory sniffing. In awake mice it is therefore the serotonergic raphe neurons that are predominant in detecting and mediating the effects of elevated inspired CO_2. Neurons of the RTN have heterogeneous roles but make relatively little contribution to this key homeostatic reflex.

One sentence summary:

Neurons of the raphe, but not the retrotrapezoid nucleus, dominate the response to inspiration of elevated CO_2 in awake adult mice.

The precise control of breathing is fundamental to the survival of all terrestrial vertebrates. Breathing fulfils two essential functions: provision of oxygen to support metabolism; and removal of the metabolic by-product, CO_2. Rapid and regulated removal of CO_2 is essential because its over-accumulation in blood will result in death from the consequent drop in pH. The CO_2-dependent regulation of breathing is mediated by chemosensitive neurons and glia in the medulla oblongata (1-3). In the rostral region of the medulla oblongata evidence favours the involvement of two neuronal populations: the Phox2B+ neurons of the retrotrapezoid nucleus (RTN) (4-8) and the serotonergic neurons of the rostral medullary raphe (9-12). Assessment of the relative roles of these two neuronal populations has been hampered by the inability to record their activity in awake freely behaving adult rodents during a hypercapnic challenge. Instead neuronal recordings have been made from young <14d or adult rodents under anaesthesia. Both of these methods have drawbacks -the chemosensory control of breathing matures postnatally; and anaesthesia is known to depress the activity of respiratory neurons.

Recently, methods have been developed to allow recording of activity of defined neuronal populations in awake, freely-moving animals (13,14). These methods require: the expression of genetically encoded Ca^{2+} indicators such as GCaMP6 in the relevant neurons; the implantation of gradient refractive index (GRIN) lenses at the correct stereotaxic position; and a head-mounted mini-epifluorescence microscope to enable image acquisition during the free behaviour of the mouse (Fig 1A). These methods have allowed imaging in deep brain structures such as the hypothalamus. We have now adapted them to enable recording of defined neuronal populations in the brainstem of mice. Neurons of the RTN were targeted with a GCaMP6 AAV, the localization of successful and accurate transduction was confirmed posthoc by using choline acetyltransferase (ChAT) staining to define the facial nucleus and the location of the transduced cells (Fig 1F). Neurons of the rostral medullary raphe were also targeted with tryptophan hydroxylase (TPH) staining used to verify accurate transduction of this structure and the presence of serotonergic neurons (Fig 1G).

We recorded 81 RTN neurons in 3 mice. Surprisingly, the responses to the hypercapnic challenge were highly variable (Fig 2A), supporting recent findings showing functional heterogeneity in the RTN (15). 3/81 neurons were inhibited by hypercapnia (Fig 2A, H, Supplementary Movie 1) and a further 3/81 exhibited Ca^{2+} transients that coincided with exploratory sniffing (Fig 2A,B,I,Supplementary Movie 1). Interestingly, neurons that exhibited the same activity patterns (i.e., CO_2-inhibited or sniff-activated neurons) were grouped in clusters (Fig 1D, 2A). Only 4/81 neurons exhibited an increase in Ca^{2+} during a hypercapnic challenge, and only to the higher level of inspired CO_2 (6%) (Fig 2C,D,G). Given the prior expectation that RTN neurons should exhibit robust changes in firing to CO_2 (6-8) the very low frequency of CO_2-activated neurons was surprising. Stimulation of sniffing leads to *c-Fos* expression in the retrofacial area of the cat (roughly equivalent to the RTN) (16), and para-ambigual expiratory and inspiratory neurons, which are respectively silenced and coactive with

sniffing have previously been described in the anesthetised cat (17). However we are the first to demonstrate a potential role for the RTN in controlling sniffing.

As the evidence for chemosensory neurons in the rostral medulla is compelling and has been amassed over many years from many independent studies (3,18-26), we next examined whether the activity of neurons in the rostral medullary raphe (i.e. raphe magnus and pallidus) could be altered by CO_2 (Fig 3). Once again we found heterogeneity of responses, but in the rostral medullary raphe a far greater proportion of neurons (19/47, 3 mice) responded to CO_2 than in the RTN (χ^2=23.06, p=0.000002). About 40% of the neurons showed an increase in Ca^{2+} to CO_2. As there are also GABAergic neurons in the raphe (27-29), we analyzed the proportion of serotonergic neurons that we transduced (Fig 3C) and found that 68% of transduced neurons were serotonergic. 4/19 responding neurons were only activated by 3% inspired CO_2 (Fig 3A,D,H, Supplementary Movie 2). The remainder showed responses at both 3 and 6% inspired CO_2, with a much greater response at 6% inspired CO_2 than at 3% (Fig 3A,G). The Ca^{2+} responses during hypercapnia also exhibited heterogeneity. Some neurons exhibited periodic Ca^{2+} transients, suggestive of burst firing (Fig 3A,B, Supplementary Movie 2), whereas others exhibited more sustained elevations of Ca^{2+} suggestive of high frequency unpatterned firing.

To gain an understanding of the relative contributions of the RTN and medullary raphe to the total chemosensory response we normalized the integrated total of the Ca^{2+} responses to the number of recorded cells in each nucleus (Fig 4A). This is valid under the simplifying assumption that each neuron has the potential to contribute the same amount to the physiological response to CO_2. This analysis suggests a much greater contribution of the raphe to the chemosensory response than the RTN. Whereas neurons in the raphe show responses to both 3 and 6% CO_2 we only observed responses in a few RTN neurons at the higher level of inspired CO_2.

Evidence for the involvement of the RTN comes mainly from neonatal or young juvenile animals (6-8). The relatively small activation of RTN neurons during hypercapnia in awake adult mice is surprising given this prior evidence. However the prior evidence depends heavily on recording neural activity in anaesthetized animals. A potential resolution of our new data with that in the literature is that we find RTN neurons, unresponsive to CO_2 in awake animals, are capable of being activated during hypercapnia under anaesthesia (Supplementary Figure S1). Furthermore, there is evidence that by about 3 months chemosensory control adapts and has much less dependence on the Phox2B+ neurons of the RTN (7).

Several lines of evidence have suggested the importance of medullary raphe serotonergic neurons in mediating respiratory chemosensitivity: the proximity of raphe neuron processes to blood vessels;

the correspondence of the location of CO_2-dependent ATP release at the medullary surface and the raphe neurons (11,25); and most compellingly the observation that inhibition of their activity via inhibitory DREADD receptors removes about 40% of the total adaptive ventilatory response in awake mice (12).

Recently the pH sensitive channel GPR4 has been claimed to endow RTN neurons with pH sensitivity (8). The extent to which GPR4 in RTN neurons contributes to respiratory chemosensitivity is the subject of conflicting evidence (30). Global knockout of GPR4 severely attenuates the adaptive response to hypercapnia (8), but this channel is widely expressed centrally and peripherally including in the carotid body chemosensory cells and the medullary raphe (8,30). Our *in vivo* recordings from freely moving mice suggest that in the rostral chemosensory area, it is the raphe neurons that play the major role in mediating chemosensitivity. That they express GPR4 suggests they possess intrinsic pH sensitivity, but given their proximity to sites of CO_2-dependent ATP release (25,26), they may also be the site of convergence of direct CO_2 sensitivity mediated via Cx26.

We therefore propose a model (Fig 4B) in which CO_2 respiratory chemosensitivity is mainly mediated by the serotonergic raphe neurons acting on the preBötzinger complex, with a contribution from RTN neurons excited by CO_2. If the CO_2-inhibited neurons of the RTN were to inhibit inspiratory neurons of the preBötzinger complex indirectly via activation (31) of inhibitory neurons in the Bötzinger complex (32,33), these RTN neurons could additionally contribute to the enhancement of breathing via CO_2-mediated disinhibition. We further propose that the sniff-activated neurons of the RTN feed excitation to inspiratory neurons of the preBötzinger complex to trigger exploratory sniffing.

References

1. Guyenet, P. G., Stornetta, R. L., and Bayliss, D. A. (2010) Central respiratory chemoreception. *The Journal of Comparative Neurology* **518**, 3883-3906
2. Nattie, E. (2011) Julius H. Comroe, Jr., Distinguished Lecture: Central chemoreception: then … and now. *Journal of Applied Physiology* **110**, 1-8
3. Huckstepp, R. T., and Dale, N. (2011) CO2-dependent opening of an inwardly rectifying K+ channel. *Pflugers Archiv : European journal of physiology* **461**, 337-344
4. Smith, J. C., Morrison, D. E., Ellenberger, H. H., Otto, M. R., and Feldman, J. L. (1989) Brainstem projections to the major respiratory neuron populations in the medulla of the cat. *J Comp Neurol* **281**, 69-96
5. Nattie, E. E., and Li, A. (1994) Retrotrapezoid nucleus lesions decrease phrenic activity and CO2 sensitivity in rats. *Respir Physiol* **97**, 63-77
6. Mulkey, D. K., Stornetta, R. L., Weston, M. C., Simmons, J. R., Parker, A., Bayliss, D. A., and Guyenet, P. G. (2004) Respiratory control by ventral surface chemoreceptor neurons in rats. *Nat Neurosci* **7**, 1360-1369
7. Ramanantsoa, N., Hirsch, M.-R., Thoby-Brisson, M., Dubreuil, V., Bouvier, J., Ruffault, P.-L., Matrot, B., Fortin, G., Brunet, J.-F., Gallego, J., and Goridis, C. (2011) Breathing without CO2 Chemosensitivity in Conditional Phox2b Mutants. *The Journal of Neuroscience* **31**, 12880-12888

8. Kumar, N. N., Velic, A., Soliz, J., Shi, Y., Li, K., Wang, S., Weaver, J. L., Sen, J., Abbott, S. B., Lazarenko, R. M., Ludwig, M. G., Perez-Reyes, E., Mohebbi, N., Bettoni, C., Gassmann, M., Suply, T., Seuwen, K., Guyenet, P. G., Wagner, C. A., and Bayliss, D. A. (2015) Regulation of breathing by CO(2) requires the proton-activated receptor GPR4 in retrotrapezoid nucleus neurons. *Science* **348**, 1255-1260
9. Richerson, G. B., Wang, W., Tiwari, J., and Bradley, S. R. (2001) Chemosensitivity of serotonergic neurons in the rostral ventral medulla. *Respir Physiol* **129**, 175-189
10. Richerson, G. B. (2004) Serotonergic neurons as carbon dioxide sensors that maintain pH homeostasis. *Nat Rev Neurosci* **5**, 449-461
11. Corcoran, A. E., Hodges, M. R., Wu, Y., Wang, W., Wylie, C. J., Deneris, E. S., and Richerson, G. B. (2009) Medullary serotonin neurons and central CO(2) chemoreception. *Respir Physiol Neurobiol*
12. Ray, R. S., Corcoran, A. E., Brust, R. D., Kim, J. C., Richerson, G. B., Nattie, E., and Dymecki, S. M. (2011) Impaired respiratory and body temperature control upon acute serotonergic neuron inhibition. *Science* **333**, 637-642
13. Ziv, Y., and Ghosh, K. K. (2015) Miniature microscopes for large-scale imaging of neuronal activity in freely behaving rodents. *Curr Opin Neurobiol* **32**, 141-147
14. Jennings, J. H., Ung, R. L., Resendez, S. L., Stamatakis, A. M., Taylor, J. G., Huang, J., Veleta, K., Kantak, P. A., Aita, M., Shilling-Scrivo, K., Ramakrishnan, C., Deisseroth, K., Otte, S., and Stuber, G. D. (2015) Visualizing hypothalamic network dynamics for appetitive and consummatory behaviors. *Cell* **160**, 516-527
15. Huckstepp, R. T. R., Cardoza, K. P., Henderson, L. E., and Feldman, J. L. (2018) Distinct parafacial regions in control of breathing in adult rats. *PLoS One* **13**, e0201485
16. Jakus, J., Halasova, E., Poliacek, I., Tomori, Z., and Stransky, A. (2004) Brainstem areas involved in the aspiration reflex: c-Fos study in anesthetized cats. *Physiological research* **53**, 703-717
17. Batsel, H. L., and Lines, A. J., Jr. (1973) Bulbar respiratory neurons participating in the sniff reflex in the cat. *Exp Neurol* **39**, 469-481
18. Mitchell, R. A., Loeschcke, H. H., Severinghaus, J. W., Richardson, B. W., and Massion, W. H. (1963) Regions of respiratory chemosensitivity on the surface of the medulla. *Ann N Y Acad Sci* **109**, 661-681
19. Loeschcke, H. H. (1982) Central chemosensitivity and the reaction theory. *J Physiol* **332**, 1-24
20. Shams, H. (1985) Differential effects of CO2 and H+ as central stimuli of respiration in the cat. *J Appl Physiol* **58**, 357-364
21. Nattie, E. (1999) CO2, brainstem chemoreceptors and breathing. *Prog Neurobiol* **59**, 299-331.
22. Nattie, E. E. (2001) Central chemosensitivity, sleep and wakefullness. *Respiration Physiology* **129**, 257-268
23. Milsom, W. K. (2002) Phylogeny of CO2/H+ chemoreception in vertebrates. *Respir Physiol Neurobiol* **131**, 29-41
24. Gourine, A. V., Kasymov, V., Marina, N., Tang, F., Figueiredo, M. F., Lane, S., Teschemacher, A. G., Spyer, K. M., Deisseroth, K., and Kasparov, S. (2010) Astrocytes control breathing through pH-dependent release of ATP. *Science* **329**, 571-575
25. Gourine, A. V., Llaudet, E., Dale, N., and Spyer, K. M. (2005) ATP is a mediator of chemosensory transduction in the central nervous system. *Nature* **436**, 108-111
26. Huckstepp, R. T., id Bihi, R., Eason, R., Spyer, K. M., Dicke, N., Willecke, K., Marina, N., Gourine, A. V., and Dale, N. (2010) Connexin hemichannel-mediated CO2-dependent release of ATP in the medulla oblongata contributes to central respiratory chemosensitivity. *J Physiol* **588**, 3901-3920
27. Calizo, L. H., Akanwa, A., Ma, X., Pan, Y. Z., Lemos, J. C., Craige, C., Heemstra, L. A., and Beck, S. G. (2011) Raphe serotonin neurons are not homogenous: electrophysiological, morphological and neurochemical evidence. *Neuropharmacology* **61**, 524-543
28. Iceman, K. E., and Harris, M. B. (2014) A group of non-serotonergic cells is CO2-stimulated in the medullary raphe. *Neuroscience* **259**, 203-213

29. Iceman, K. E., Corcoran, A. E., Taylor, B. E., and Harris, M. B. (2014) CO2-inhibited neurons in the medullary raphe are GABAergic. *Respir Physiol Neurobiol* **203**, 28-34
30. Hosford, P. S., Mosienko, V., Kishi, K., Jurisic, G., Seuwen, K., Kinzel, B., Ludwig, M. G., Wells, J. A., Christie, I. N., Koolen, L., Abdala, A. P., Liu, B. H., Gourine, A. V., Teschemacher, A. G., and Kasparov, S. (2018) CNS distribution, signalling properties and central effects of G-protein coupled receptor 4. *Neuropharmacology* **138**, 381-392
31. Rosin, D. L., Chang, D. A., and Guyenet, P. G. (2006) Afferent and efferent connections of the rat retrotrapezoid nucleus. *J Comp Neurol* **499**, 64-89
32. Ezure, K., and Manabe, M. (1988) Decrementing expiratory neurons of the Botzinger complex. II. Direct inhibitory synaptic linkage with ventral respiratory group neurons. *Exp Brain Res* **72**, 159-166
33. Richter, D. W., and Smith, J. C. (2014) Respiratory rhythm generation in vivo. *Physiology (Bethesda)* **29**, 58-71

Acknowledgements

Funding: This work was supported by an MRC Discovery Award MC_PC_15070. ND is a Royal Society Wolfson Research Merit Award Holder.

Author contributions:
AB performed the experiments and analyzed the data; RH designed and oversaw the surgical aspects of the study; ND conceived and designed the study; all authors reviewed the data and contributed to writing of the manuscript.

Competing interests: The authors declare that they have no competing interests.

Data and Materials availability: Raw data available on request.

List of Supplementary Materials

Materials and Methods
Supplementary Figure S1
Supplementary Movie 1
Supplementary Movie 2

Figures and Legends

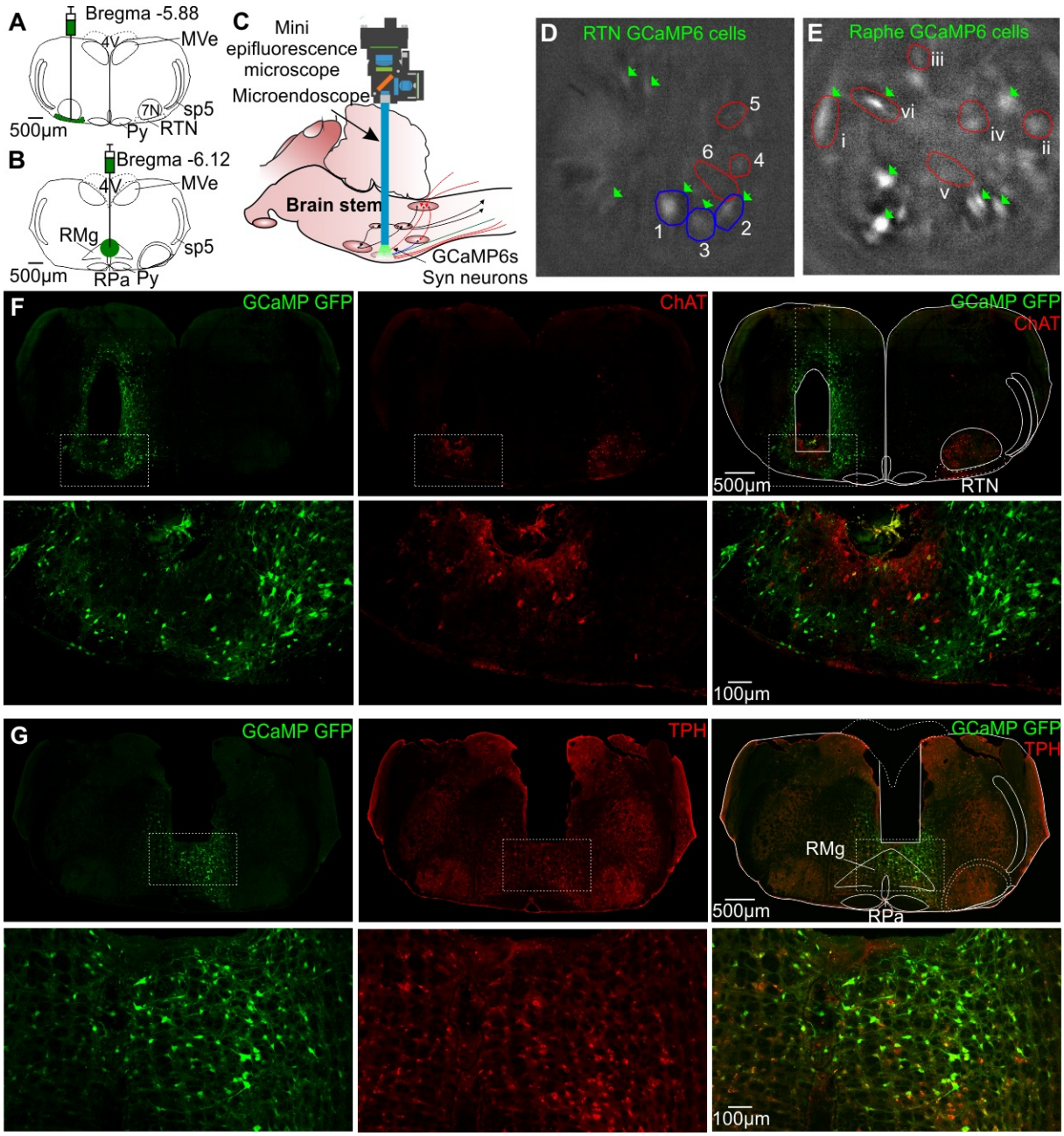

Figure 1. Viral transfection and GRIN lens implantation in the RTN or rostral medullary raphe. (A) AAV9-GCaMP6s injection into (A) the RTN (Bregma -5.88mm) and (B) the rostral medullary raphe (Bregma -6.12mm). 7N, facial motor nucleus; Py, pyramidal tract; MVe, medial vestibular nucleus; sp5, spinal trigeminal nucleus. (C) Representation of GRIN lens (microendoscope) placement into the RTN or medullary raphe along with baseplate implantation and placement of mini epifluorescence camera. (D) Ca^{2+} fluorescence signal from GCaMP6s transfected RTN neurons in freely behaving mice. 1,2 and 3, individual regions of interest (ROIs) drawn around neurons inhibited during 3% and 6% CO_2 response; 4,5 and 6, ROIs drawn around neurons coactivated with sniff/exploratory behaviour. These numbers correspond to the numbered traces in Fig 2A. (E) Ca^{2+} signal from GCaMP6s transfected medullary raphe neurons in freely behaving mouse. ROIs i-vi,

indicate medullary raphe neurons responding to 3% and 6% CO_2. (F) Histology of brainstem section from the mouse recorded for the RTN. Top panel shows the native GCaMP6 staining (green), ChAT immunostaining (red) and merge of GCaMP6 and ChAT along with the GRIN lens tract (solid line is the lens track in the sectioned tissue extended out to the dorsal surface as a dotted line). Dotted squares are expanded in the bottom panel showing the GCaMP6 and ChAT positive neurons and their merge. (G) Histology of brainstem section from the mouse recorded for the medullary raphe. Top panel shows the native GCaMP6 staining (green), TPH (marker for serotonergic neurons) immunostaining (red) and merge of GCaMP6 and TPH along with the GRIN lens track (solid line). Dotted squares are expanded in the bottom panel showing the GCaMP6 and TPH stained neurons and their merge. RMg, Raphe magnus.

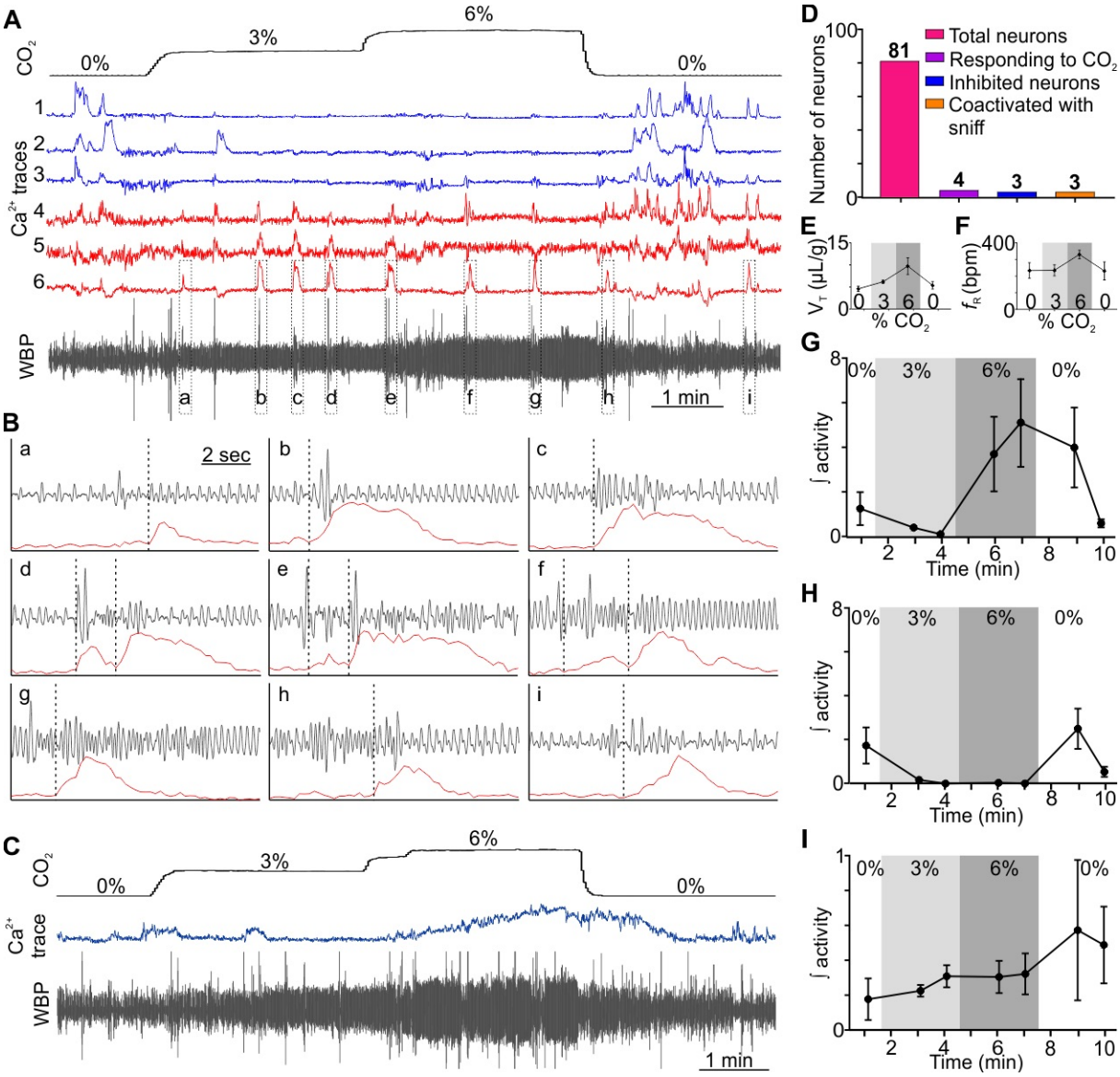

Figure 2. Responses of the RTN neurons to elevated inspired CO_2 are heterogeneous. (A) Recording of mouse whole body plethysmography (WBP) (bottom panel) in response to changes in

CO_2 in plethysmography chamber (top panel) is time-matched with the Ca^{2+} signals from RTN neurons (middle panel). Calcium traces 1-6 correspond to the neurons shown in Fig 1D. Ca^{2+} signals were extracted from ROIs and equally scaled on the y-axis. Blue Ca^{2+} traces (1-3) showing the RTN neurons inhibited during both 3% and 6% CO_2 stimulus. Red Ca^{2+} traces (4-6) show the neurons coactivated with exploratory sniffing behaviour (confirmed by video recording). The dotted squares (a-i) are individual Ca^{2+} events (action potential) from single neuron (ROI) time matched with WBP and expanded in Ba-i. (B) The start of the Ca^{2+} transient is shown by the dotted line. (C) Ca^{2+} trace of a CO_2-responsive RTN neuron matched with the WBP and % CO_2 trace. (D) Proportions of the different responses observed in RTN neurons recorded from three mice. (E-F) Change in breathing frequency, f_R (breaths per minute (bpm)) and tidal volume, V_T (μL/g) in response to change in CO_2 concentration in RTN recorded mice. (G) Activity of the RTN neurons responded to 6% CO_2. (H) Changes in activity of RTN neurons inhibited during CO_2 response. (I) Activity of sniff-activated RTN neurons shows no correlation with CO_2 levels during CO_2 response. In panel G-I, X-axis is the time at which area under curve (60sec) of Ca^{2+} activity is calculated. Y-axis is arbitrary units of integrated Ca^{2+} activity.

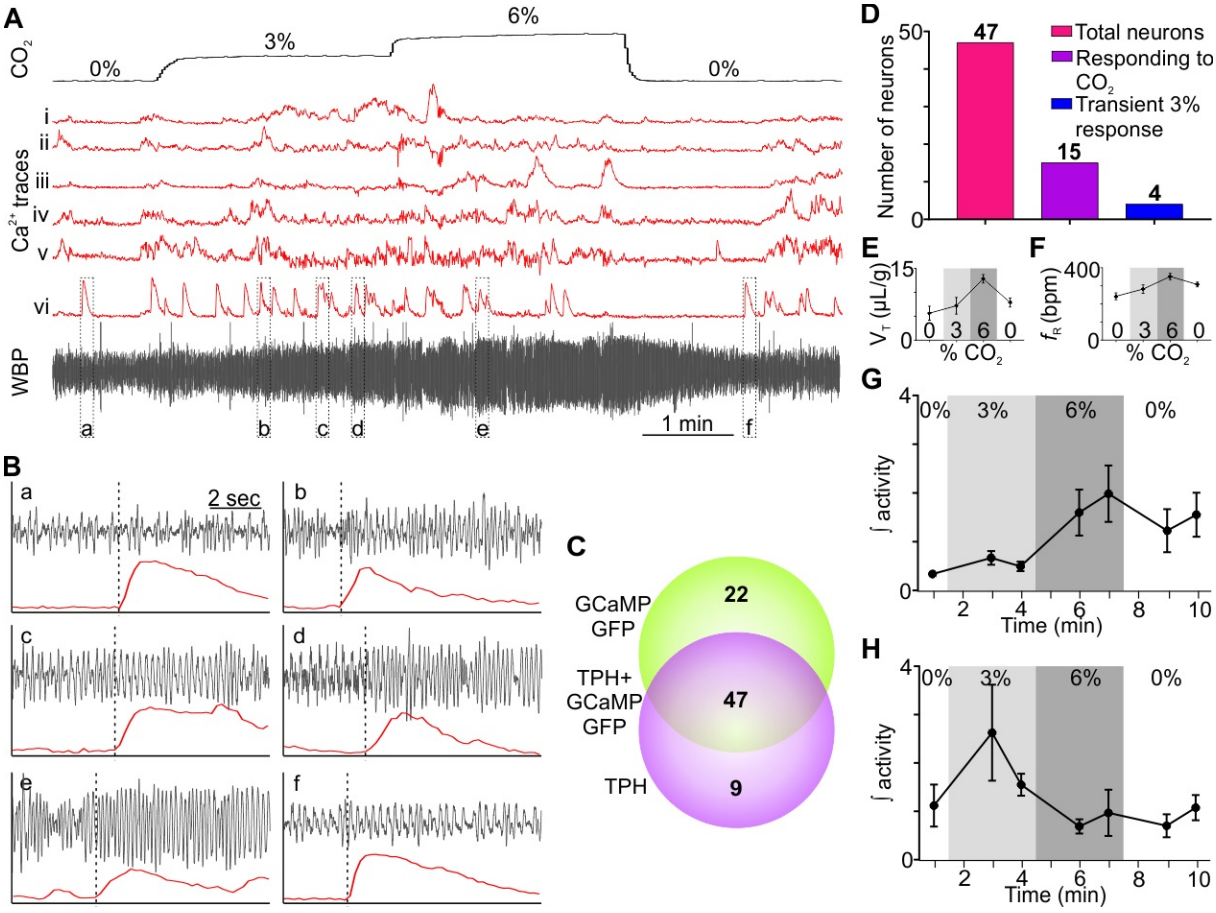

Figure 3. Serotonergic medullary raphe neurons are predominant in detecting elevated inspired CO_2. (A) Ca^{2+} activity of raphe neurons recorded simultaneously with WBP responses to

hypercapnia. The Ca^{2+} signals were extracted from ROIs and equally scaled on the y-axis. Individual Ca^{2+} traces (i-vi) show the activated neurons and their responses to CO_2 (and correspond to equivalently labelled ROIs in Fig 1E). Dotted squares (a-f) represent the individual Ca^{2+} events from a single neuron (ROI) time matched with WBP and expanded in Ba-f. (B) Almost all Ca^{2+} events are associated with either changes in breathing frequency or tidal volume. (C) The colocalization GCaMP6s transfected neurons within the field of view of the GRIN lens (200μm below the lens surface) with serotonergic neurons in the raphe (600 X 400 μm section). (D) The proportion of raphe neurons recorded from three mice that responded to CO_2. (E-F) Change in breathing frequency, f_R (bpm) and tidal volume, V_T in response to change in CO_2 concentration in raphe recorded mice. (G) Graded response of raphe neurons to 3% and 6% CO_2. (H) Changes in activity of transiently activated raphe neurons during 3% CO_2 response. In panel G-H, X-axis is the time at which area under curve (60sec) of Ca^{2+} activity is calculated. Y-axis is arbitrary units of integrated Ca^{2+} activity.

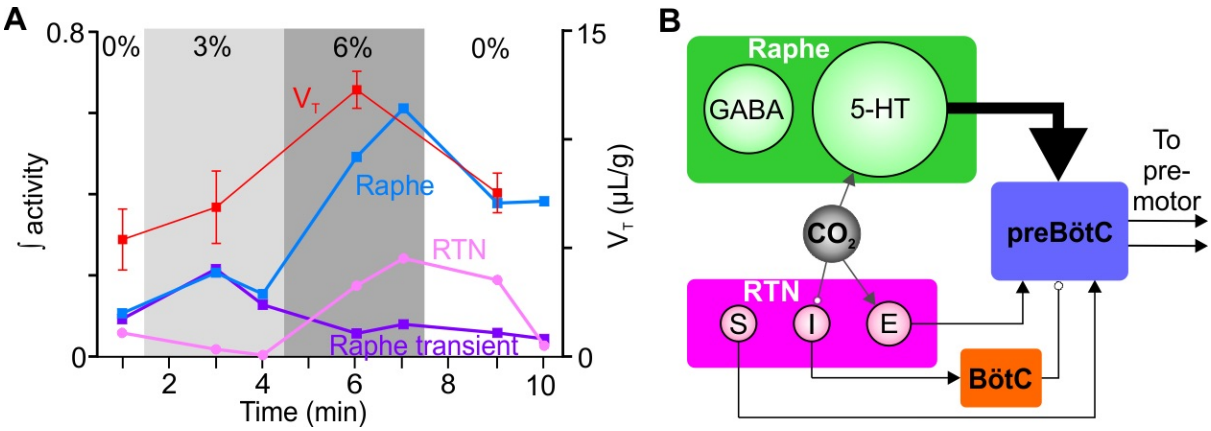

Figure 4. Weighted responses of RTN vs raphe nuclei to elevated CO_2 and model for the contributions of the RTN and raphe to respiratory chemosensitivity. (A) Integrated Ca^{2+} responses of RTN and raphe neurons are summed separately and divided by the total number of neurons in that group to calculate the relative contribution of RTN and raphe nuclei to CO_2 chemosensitivity based on the assumption that each neuron is equally important. Tidal volume changes due to CO_2 response are shown in red (V_T). At 3% CO_2, both the raphe graded and raphe transient responses are higher than RTN responses and at 6% CO_2, raphe graded response is significantly bigger than the RTN response. X-axis is the time at which area under curve (60sec) of Ca^{2+} activity is calculated. Left Y-axis is arbitrary units of integrated Ca^{2+} activity and right Y-axis is breathing tidal volume. (B) CO_2 predominantly excites serotonergic (5-HT) raphe neurons and a very small proportion of the RTN "E" neurons. CO_2 inhibits some neurons ("I") in the RTN. We propose that the "I" neurons activate Bötzinger (BötC) neurons which inhibit the preBötC. CO_2-mediated inhibition of the RTN "I" neurons may therefore result in disinhibition of preBötC neurons. The RTN contains sniff-activated neurons ("S"), which we propose project to the preBötC.

Materials and Methods

Experiments were performed in accordance with the European Commission Directive 2010/63/EU (European Convention for the Protection of Vertebrate Animals used for Experimental and Other Scientific Purposes) and the United Kingdom Home Office (Scientific Procedures) Act (1986) with project approval from the University of Warwick's AWERB.

Viral handling

AAV-9: pGP-AAV-syn-GCaMP6s-WPRE.4.641 (Addgene, Watertown, MA, USA) at a titre of $1x10^{13}$ vp ml^{-1}. The viruses were aliquoted, and stored at -80°C. On the day of injection, viruses were removed and held at 4°C, loaded into graduated glass pipettes (Drummond Scientific Company, Broomall, PA, USA), and placed into an electrode holder for pressure injection. The vector uses synapsin promoter, and therefore transduced neurons showing higher tropism for the AAV 2/9 subtype, but not non-neuronal cells or neurons that do not show tropism for AAV 2/9 within the injection site, e.g., facial motoneurons.

Viral transfection of RTN and Raphe

Adult male C57BL/6 mice (20-30 g) were anesthetized with isofluorane (Piramal Healthcare Ltd, Mumbai, India) with concentrations varied (0.5-2.5% in pure oxygen at 1.5 L/min) to maintain adequate anaesthesia throughout the surgery. Mice received a presurgical injection of atropine (120 µg/kg; Westward Pharmaceutical Co., Eatontown, NJ, USA) and meloxicam (2 mg/kg; Norbrook Inc., Lenexa, KS, USA), subcutaneously. Mice were placed in a prone position into a digital stereotaxic apparatus (Kopf Instruments, Tujunga, CA, USA) on a heating pad (TCAT 2-LV: Physitemp, Clifton, NJ, USA) and body temperature was maintained at a minimum of 33°C via a thermocouple. The head was levelled and graduated glass pipettes containing the virus were placed stereotaxically into either the RTN or rostral medullary raphe (Fig 1A,B). The RTN was defined as the area ventral to the caudal half of the facial nucleus, between the pyramidal tract and the spinal trigeminal tract (coordinates: -1.0 mm lateral and -5.6 mm caudal from Bregma, and -5.5 mm ventral from the surface of the cerebellum; Fig 1A,F). The Raphe were defined as the medial, tryptophan hydroxylase (TPH) containing regions directly above the pyramidal tracts, level with the caudal face of the facial nucleus (coordinates: 0 mm lateral and -5.8 mm caudal from Bregma, and -5.2 mm ventral from the surface of the cerebellum; Fig 1B,G). The virus solutions were pressure injected (<300 nL) unilaterally. Pipettes were left in place for 3-5 minutes to prevent back flow of the virus solution up the pipette track. Postoperatively, mice received buprenorphine (100 µg/kg; Reckitt Benckiser, Slough, UK) intraperitoneally. Mice were allowed 2 weeks for recovery and viral expression, with food and water *ad libitum*.

GRIN lens implantation

Mice expressing GCaMP6 were anesthetized with isofluorane, given pre-surgical drugs, and placed into a stereotax as described above. The head was levelled and a glass pipette followed by a blunted hypodermic needle were inserted down the GRIN lens path to a depth 200 µm above where the lens would terminated, both were left in place for 3 mins. The GRIN lens (600 µm diameter, 7.3 mm length; Inscopix, Palo Alto, CA, USA) was then inserted to a depth ~300 µm above the RTN or raphe (coordinates: RTN – 1.1 mm lateral and -5.75 mm caudal from Bregma, and -5.3 mm ventral from the surface of the cerebellum; Raphe - 0 mm lateral and -5.95 mm caudal from Bregma, and -5.1 mm ventral from the surface of the cerebellum). The lens was then secured in place with SuperBond™ (Prestige Dental, Bradford, UK). Postoperatively, mice received buprenorphine, and were allowed 2 weeks for recovery, with food and water *ad libitum*.

Baseplate installation

Mice expressing GCaMP6 and implanted with GRIN lens were anesthetized with isofluorane, given pre-surgical drugs, and placed into a stereotax as described above. To hold the miniaturized microscope during recordings, a baseplate was positioned over the lens and adjusted until the cells under the GRIN lens were in focus. The baseplate was them secured with superbond™, and coated in black dental cement (Vertex Dental, Soesterberg, the Netherlands) to stop interference of the recording from ambient light. Mice were allowed 1 week for recovery, with food and water *ad libitum*.

Freely Moving Ca^{2+} Imaging

All mice were trained with dummy camera and habituated to plethysmography chamber at least twice before imaging. The miniature microscope with integrated 475 nm LED (Inscopix, Palo Alto, CA, USA) was secured to the baseplate. GCaMP6 fluorescence was visualised through the GRIN lens, using nVista 2 HD acquisition software (Inscopix, Palo Alto, CA, USA). Calcium fluorescence was optimised for each experiment so that the histogram range was ~150-600, with average recording parameters set at 20 frames/sec with the LED power set to 15 mW of light and a digital gain of 1.0. A TTL pulse was used to synchronize the calcium signalling to the plethysmography trace. All images were processed using inscopix data processing software (Inscopix, Palo Alto, CA, USA).

Plethysmography

Mice were placed into a custom-made plethysmography chamber. The chamber was ~0.5 L with an airflow rate of 1 l min^{-1}. The plethysmography chamber was heated to 31^{o}C (thermoneutral for C57/Bl6 mice). CO_2 concentrations were sampled via a Hitech Intruments (Luton, UK) GIR250 Dual Sensor Gas analyzer connected to the inflow immediately before entering the chamber. The analyser had a delay of ~15-20 sec to read-out the digital output of gas mixture as can be seen in Fig 2A, C and 3A). Pressure transducer signals and CO_2 measurements were amplified and filtered using the NeuroLog system (Digitimer, Welwyn Garden City, UK) connected to a 1401 interface and acquired on a computer using *Spike2* software (Cambridge Electronic Design, Cambridge, UK)). Video data

was recorded with *Spike2* software and was synchronised with the breathing trace. Airflow measurements were used to calculate: tidal volume (V_T: signal trough at the end of expiration subtracted from the peak signal during inspiration, converted to mL following calibration), and respiratory frequency (F_R: breaths per minute).

Hypercapnia in freely behaving mice

Instrumented mice were placed into the plethysmograph and allowed ~30 mins to acclimate to the chamber. The LED was activated through TTL pulse synchronised with the *Spike2* recording and a 1 min of baseline recordings were taken (gas mixture: 0% CO_2 21% O_2 79% N_2). The mice were then exposed to 3 min epochs of hypercapnic gas mixture at 2 concentrations of CO_2 (3 and 6%, in 21% O_2 balanced N_2), the order of which was randomised for each experiment. Following exposure to the hypercapnic gas mixtures, CO_2 levels were reduced back to 0% and calcium signals were recorded for a further 3 minute recovery period.

Hypercapnia in urethane anaesthetised mice

Instrumented mice were anaesthetised with and IP injection of 1.2-1.5 g/kg urethane (Sigma-Aldrich, St Louis, MO, USA) and placed into the plethysmograph. Raphe recordings used an identical protocol to the awake freely behaving mice (see above). For RTN neurons, the LED was activated and 3 minutes of baseline recording were taken. The mice were then exposed to 2-minute epochs of hypercapnic gas mixture 3% and 6% (in 21% O_2 balanced N_2). Mice were then exposed to a 3-minute epoch of 9% CO_2 (in 21% O_2 balanced N_2), as experiments into the chemosensitivity of RTN neurons in mice often use 6% CO_2 in freely behaving experiments but 9% CO_2 in anaesthetised animals. Following exposure to the hypercapnic gas mixtures, CO_2 levels were reduced back to 0% and calcium signals were recorded for a further 3-minute recovery period.

Immunocytochemistry

Mice were humanely killed by pentobarbital overdose (>100 $mg \cdot kg^{-1}$) and transcardially perfused with paraformaldehyde solution (4% PFA; Sigma-Aldrich, St Louis, MO, USA). The head was removed and postfixed in PFA (4 °C) for 3 days to preserve the lens tract. The brains were removed and postfixed in PFA (4 °C) overnight. Brainstems were serially sectioned at 70 µm. Free-floating sections were incubated for 1 hour in a blocking solution (PBS containing 0.1% Triton X-100 and 5% BSA). Primary antibodies (goat anti-cholineacetyl transferase [ChAT; 1:100; Millipore, Burlington, MA, USA], or rabbit anti-tryptophan hydroxylase [TPH; 1:500; Sigma-Aldrich, St Louis, MO, USA] antibody) were added and tissue was incubated overnight at room temperature. Slices were washed in PBS (6 × 5 mins) and then incubated for 2-4 hours in a blocking solution with the secondary antibodies: either donkey anti-rabbit Alexa Fluor 568 (1:250; Jackson Laboratory, Bar Harbor, ME, USA), or donkey anti-Goat Alexa Cy3 (1:250; Jackson Laboratory, Bar Harbor, ME, USA) antibody, tissue was then incubated for 2-4 hours at room

temperature. Tissue was washed in PBS (6 × 5 min). Slices were mounted, coverslipped and examined using a Zeiss 880 confocal microscope with ZEN aquisition software (Zeiss, Oberkochen, Germany).

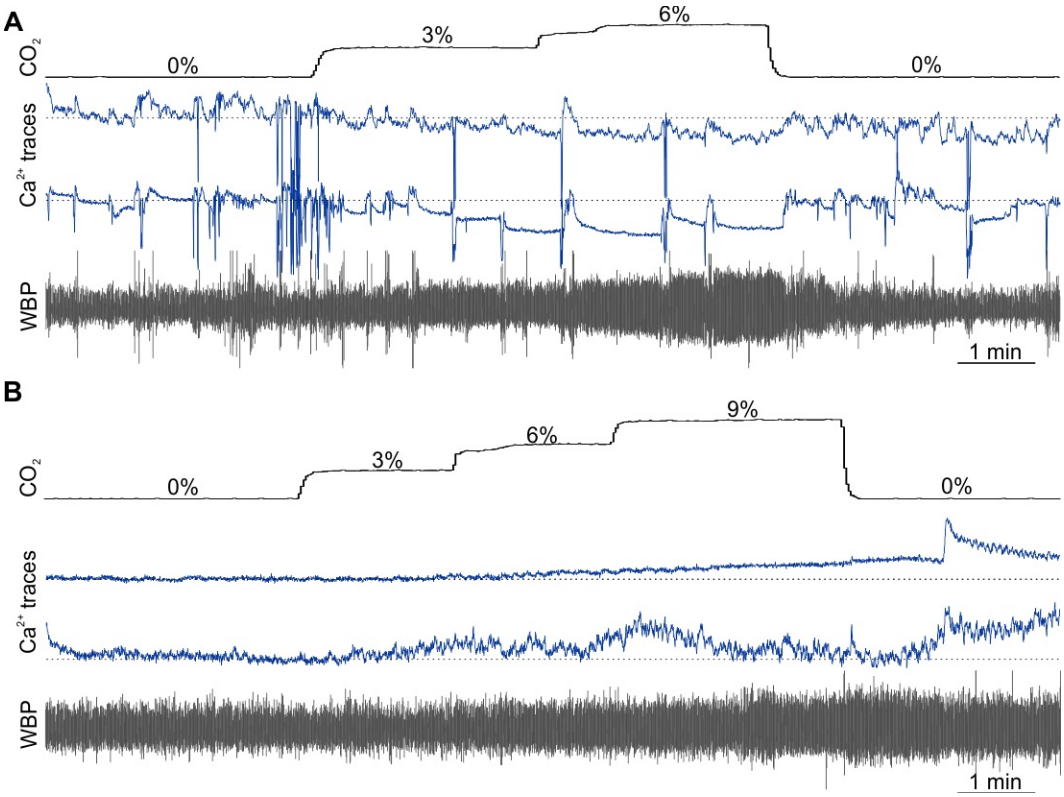

Supplementary Figure S1. Anaesthesia alters the response of RTN neurons to CO_2. A) In an awake animal two RTN neurons did not exhibit any responses to CO_2 and their baseline Ca^{2+} levels were reduced by elevated CO_2. Ca^{2+} traces from two neurons shown along with whole body plethysmographys traces (WBP). The large positive and negative transients are movement artefacts and not Ca^{2+} signals. Movement artefacts were sufficiently problematic that no data was used from this mouse while awake. B) Under urethane anaesthesia (and hence no movement), the same two neurons exhibited a gradual increase in Ca^{2+} during hypercapnia. Note that the response to hypercapnia under anesthesia is much weaker than when awake and required higher levels of CO_2 to evoke an increase in breathing than in the awake state (compare to A).